Nonlinear Analysis: Modelling and Control, Online First, 1–17
https://doi.org/10.15388/namc.2025.30.43741

Vilnius University Press

A new dynamic model for simultaneous saccharification and fermentation process of rice wine*

Li Wang, Lihong Zhang, Tingting Guan

Shanxi Key Laboratory of Cryptography and Data Security,
School of Mathematical Sciences, Shanxi Normal University,
Taiyuan, Shanxi 030031, China
wangl3967@163.com; zhanglih149@126.com;
guantingting1985@163.com

Received: July 5, 2024 / **Revised:** July 18, 2025 / **Published online:** October 7, 2025

Abstract. In this paper, a new fractional model for the simultaneous saccharification and fermentation process of rice wine is proposed. To begin with, the existence and uniqueness of solution to the new model are proved by using some fixed point theorems. In addition, the stability at the equilibrium point and the Ulam–Hyers stability of the fractional simultaneous and saccharification fermentation model are analyzed. Then the approximate solutions of the fractional simultaneous saccharification and fermentation model are obtained by using the generalised Euler method. Finally, numerical simulations are given to verify the rationality of the fractional simultaneous saccharification and fermentation model. The new model proposed in this paper can more sensitively capture changes in the reaction.

Keywords: simultaneous saccharification and fermentation, fixed point theorem, stability analysis, generalized Euler method, numerical simulation.

1 Introduction

Rice wine, a traditional fermented wine, has a long history and deep cultural background in China [23]. It is rich in nutrients, containing a small amount of protein, glucose, fructose, sucrose, vitamins B and C, etc. [17, 19, 21]. Rice wine is made by adding wheat Qu and yeast to steamed glutinous rice or rice, where steamed glutinous rice replaces starch as the basic material, and wheat Qu replaces purifying enzymes [24]. The fermentation process of rice wine includes initial fermentation stage and post-fermentation stage. In the initial fermentation stage, the saccharification of starch and the fermentation of sugar take place simultaneously, which is called as simultaneous saccharification and fermentation (SSF) [8]. It protects the yeast cells from high concentrations of sugar and helps produce high quality ethanol. The post-fermentation stage refers to the process

*The work is supported by the Graduate Education Innovation Program of Shanxi, China (No. 2024JG103).

in which microorganisms continue to ferment to improve the taste of rice wine after the initial fermentation process is completed. This paper focuses on the initial fermentation stage of rice wine.

Fractional calculus is widely used in many fields such as physics [4], signal processing [26], biomedical engineering [11], and so on. In 2017, Singh et al. [14] established a new smoking cessation model with fractional derivatives and demonstrated the existence and uniqueness of the solution of the model. Subsequently, they used the iterative perturbation method to obtain the solution of the model. Finally, numerical simulations were presented to prove that the fractional derivatives are very important to simulate real-world problems. In 2020, Zhang et al. [25] studied a Caputo–Hadamard-type fractional turbulence flow model by using the method of upper and lower solutions combined with monotonic iteration technique. In 2022, Wu et al. [20] used Caputo fractional derivative to establish a general plastic model for rockfill materials. They used the proposed model to simulate drainage triaxial compression tests of five rockfill materials. By comparing the test results and simulation results, it is obtained that the proposed model can effectively simulate the stress and strain behavior of rockfill materials. In 2024, Huang et al. [3] proposed a new fractional wine fermentation model and made qualitative analysis and numerical simulation for the new model. They show the advantages of the proposed fractional wine fermentation model, which provides the optimal strategy for the control of heat in the production process, which further provides a good support for the high-quality production of wine. To sum up, fractional derivatives help us to better understand and describe complex behaviour in systems. The advantages of fractional derivatives such as "memory" and "heritability" make it possible to better describe the SSF process of rice wine. Among them, the Caputo derivative has significant advantages. Its initial conditions are consistent with those of integer-order differential equations, offering clear interpretations and facilitating the connection with practical problems. Additionally, it performs excellently in characterizing complex systems with memory and hereditary properties. The Caputo fractional derivative of a function $N(t)$ with order η is defined to be

$$ {}^{C}D_t^{\eta} N(t) = \frac{1}{\Gamma(n-\eta)} \int_0^t N^{(n)}(\xi)(t-\xi)^{n-\eta-1}\,\mathrm{d}\xi, $$

where $n-1 < \eta \leqslant n$, $n \in \mathbb{N}$. Based on this, we will establish a fractional SSF model and study its related properties.

Currently, some dynamic models of the SSF process for ethanol production have been established. In 2006, Kroumov et al. [7] established a two-hierarchic-level unstructured model of transgenic Saccharomyces cerevisiae YPB-G SSF process for ethanol production. In 2007, Ochoa et al. [10] studied the SSF process of the recombinant Saccharomyces cerevisiae strain to produce ethanol. Then they proposed an unstructured model and a cybernetic model to describe the process. In 2014, Wang et al. [18] studied the process of ethanol production by simultaneous saccharification co-fermentation in batches with complementary material of birch wood. They established a dynamic model to simulate the process well. In 2015, Liu et al. [9] conducted rice wine experiments at

different temperatures. Then they proposed a dynamic model with adjustable parameters for the SSF process in the rice wine experiment. Subsequently, they compared the simulation results of the model with the experimental results at different temperatures. Finally, it was concluded that the proposed model can effectively describe the dynamic behavior of the rice wine SSF process.

Although the integer-order model [9] for describing the SSF process of rice wine has been proposed and numerical simulations have been carried out, there is still some meaningful work that needs to be supplemented and improved such as optimization of the model, existence and uniqueness of the solution, and stability analysis. In this context, taking into account the advantages of fractional derivatives, inspired by the models mentioned above, this paper extends the integer-order model [9] to the fractional SSF model (1). Subsequently, the existence and uniqueness of the solution of fractional SSF model and the stability of the model are analyzed. Finally, numerical simulations of the fractional SSF model are presented. Our work not only fills the theoretical knowledge gap in the SSF process of rice wine, but also provides guidance for rice wine brewers to produce high-quality rice wine.

Since in our applications $\mathrm{d}/\mathrm{d}t$ has the unit of hour^{-1}, $\mathrm{d}^\eta/\mathrm{d}t^\eta$ has the unit of hour$^{-\eta}$, taking $0 < \eta \leqslant 1$ and τ a parameter that possesses the dimension of hour, then the unit of $[(1/\tau^{1-\eta})\mathrm{d}^\eta/\mathrm{d}t^\eta]$ is hour^{-1}. Therefore, the fractional form of the integer-order model in [9] can be introduced in the following way:

$$
\begin{aligned}
\frac{1}{\tau^{1-\eta}}{}^{C}D_t^\eta S(t) &= -\overline{k_1}SE,\\
\frac{1}{\tau^{1-\eta}}{}^{C}D_t^\eta R(t) &= \overline{k_{10}}F - \overline{k_5}\frac{R}{K_{s1}+R}\frac{O}{K_{s2}+O}C,\\
\frac{1}{\tau^{1-\eta}}{}^{C}D_t^\eta M(t) &= \overline{k_{11}}F - \overline{k_6}\frac{M}{K_{s3}+M}\frac{O}{K_{s2}+O}C - \overline{k_7}\frac{M}{K_{s4}+M}C,\\
\frac{1}{\tau^{1-\eta}}{}^{C}D_t^\eta G(t) &= \overline{k_{12}}F - \overline{k_8}\frac{G}{K_{s5}+G}\frac{O}{K_{s2}+O}C - \overline{k_9}\frac{G}{K_{s6}+G}C,\\
\frac{1}{\tau^{1-\eta}}{}^{C}D_t^\eta C(t) &= \overline{k_{13}}\frac{R}{K_{s1}+R}\frac{O}{K_{s2}+O}C + \overline{k_{14}}\frac{M}{K_{s3}+M}\frac{O}{K_{s2}+O}C\\
&\quad + \overline{k_{15}}\frac{G}{K_{s5}+G}\frac{O}{K_{s2}+O}C,\\
\frac{1}{\tau^{1-\eta}}{}^{C}D_t^\eta A(t) &= \overline{k_{16}}\frac{M}{K_{s4}+M}C + \overline{k_{17}}\frac{G}{K_{s6}+G}C,\\
\frac{1}{\tau^{1-\eta}}{}^{C}D_t^\eta O(t) &= -\overline{k_5}\frac{R}{K_{s1}+R}\frac{O}{K_{s2}+O}C - \overline{k_6}\frac{M}{K_{s3}+M}\frac{O}{K_{s2}+O}C\\
&\quad - \overline{k_8}\frac{G}{K_{s5}+G}\frac{O}{K_{s2}+O}C + O_{in},\\
\frac{1}{\tau^{1-\eta}}{}^{C}D_t^\eta E(t) &= -\overline{k_1}SE + (\overline{k_2}+\overline{k_3}+\overline{k_4})F,\\
\frac{1}{\tau^{1-\eta}}{}^{C}D_t^\eta F(t) &= \overline{k_1}SE - (\overline{k_2}+\overline{k_3}+\overline{k_4})F.
\end{aligned}
$$

Table 1. The symbols for the concentration of the different materials.

Symbol	Material	Symbol	Material
S	starch	E	wheat Qu
R	maltotriose	C	yeast cells
M	maltose	O	oxygen
G	glucose	A	ethanol
F	starch-Qu comple		

If $k = \tau^{1-\eta}\bar{k}$, for every constant k, the new fractional SSF model proposed in this paper can be written as

$$
\begin{aligned}
{}^{C}D_t^{\eta} S(t) &= -k_1 SE,\\
{}^{C}D_t^{\eta} R(t) &= k_{10}F - k_5 \frac{R}{K_{s1}+R}\frac{O}{K_{s2}+O}C,\\
{}^{C}D_t^{\eta} M(t) &= k_{11}F - k_6 \frac{M}{K_{s3}+M}\frac{O}{K_{s2}+O}C - k_7 \frac{M}{K_{s4}+M}C,\\
{}^{C}D_t^{\eta} G(t) &= k_{12}F - k_8 \frac{G}{K_{s5}+G}\frac{O}{K_{s2}+O}C - k_9 \frac{G}{K_{s6}+G}C,\\
{}^{C}D_t^{\eta} C(t) &= k_{13} \frac{R}{K_{s1}+R}\frac{O}{K_{s2}+O}C + k_{14} \frac{M}{K_{s3}+M}\frac{O}{K_{s2}+O}C\\
&\quad + k_{15} \frac{G}{K_{s5}+G}\frac{O}{K_{s2}+O}C,\\
{}^{C}D_t^{\eta} A(t) &= k_{16} \frac{M}{K_{s4}+M}C + k_{17} \frac{G}{K_{s6}+G}C,\\
{}^{C}D_t^{\eta} O(t) &= -k_5 \frac{R}{K_{s1}+R}\frac{O}{K_{s2}+O}C - k_6 \frac{M}{K_{s3}+M}\frac{O}{K_{s2}+O}C\\
&\quad - k_8 \frac{G}{K_{s5}+G}\frac{O}{K_{s2}+O}C + O_{in},\\
{}^{C}D_t^{\eta} E(t) &= -k_1 SE + (k_2+k_3+k_4)F,\\
{}^{C}D_t^{\eta} F(t) &= k_1 SE - (k_2+k_3+k_4)F
\end{aligned}
\tag{1}
$$

with initial conditions

$$
\begin{aligned}
&S(0) = S_0 \geqslant 0, \qquad R(0) = R_0 \geqslant 0, \qquad M(0) = M_0 \geqslant 0,\\
&G(0) = G_0 \geqslant 0, \qquad C(0) = C_0 \geqslant 0, \qquad A(0) = A_0 \geqslant 0,\\
&O(0) = O_0 \geqslant 0, \qquad E(0) = E_0 \geqslant 0, \qquad F(0) = F_0 \geqslant 0.
\end{aligned}
$$

The symbols for the concentrations of the different substances are given in Table 1.

Here $K_{s1} \sim K_{s6}$ are the half-saturation constants, and O_{in} is the rate of dissolved oxygen addition [9]. $k_1 \sim k_{17}$ are the reaction rate. The main products of this reaction are maltotriose, maltose, glucose, and ethanol. Starch–Qu complex is combined by starch and Qu at the rate of k_1. The starch in Starch–Qu complex is decomposed into maltotriose,

maltose, and glucose at rates of k_2, k_3, and k_4, respectively. Meanwhile, maltotriose, maltose, and glucose provide carbon sources for yeast growth at rates of k_5, k_6, and k_8, respectively. Maltose and glucose are metabolized into ethanol at rates of k_7 and k_9. Maltotriose is consumed for yeast growth and maintenance, but it is not metabolized into ethanol.

The structure of this paper is as follows. In Section 2, the existence and uniqueness of the solution for the fractional SSF model and the stability of the model are analysed. In Section 3, the numerical simulations of the fractional SSF model are presented. Conclusions are presented in Section 4.

2 Existence, uniqueness, and stability analysis

This section first presents the existence and uniqueness of the solution for the fractional SSF model and then analyzes the stability at the equilibrium point and the Ulam–Hyers stability of the fractional SSF model.

In the fractional SSF model (1), let

$$
\begin{aligned}
\Theta_1 &= -k_1 SE,\\
\Theta_2 &= k_{10}F - k_5 \frac{R}{K_{s1}+R}\frac{O}{K_{s2}+O}C,\\
\Theta_3 &= k_{11}F - k_6 \frac{M}{K_{s3}+M}\frac{O}{K_{s2}+O}C - k_7 \frac{M}{K_{s4}+M}C,\\
\Theta_4 &= k_{12}F - k_8 \frac{G}{K_{s5}+G}\frac{O}{K_{s2}+O}C - k_9 \frac{G}{K_{s6}+G}C,\\
\Theta_5 &= k_{13}\frac{R}{K_{s1}+R}\frac{O}{K_{s2}+O}C + k_{14}\frac{M}{K_{s3}+M}\frac{O}{K_{s2}+O}C\\
&\quad + k_{15}\frac{G}{K_{s5}+G}\frac{O}{K_{s2}+O}C,\\
\Theta_6 &= k_{16}\frac{M}{K_{s4}+M}C + k_{17}\frac{G}{K_{s6}+G}C,\\
\Theta_7 &= -k_5 \frac{R}{K_{s1}+R}\frac{O}{K_{s2}+O}C - k_6 \frac{M}{K_{s3}+M}\frac{O}{K_{s2}+O}C\\
&\quad - k_8 \frac{G}{K_{s5}+G}\frac{O}{K_{s2}+O}C + O_{in},\\
\Theta_8 &= -k_1 SE + (k_2+k_3+k_4)F,\\
\Theta_9 &= k_1 SE - (k_2+k_3+k_4)F.
\end{aligned}
$$

Then model (1) can be written as

$$
\begin{aligned}
&{}^{C}D^{\eta}N(t) = \Phi\big(t, N(t)\big), \quad 0 < \eta \leqslant 1,\\
&N(0) = N_0,
\end{aligned}
\tag{2}
$$

where $t \in [0,T]$ and

$$N(t) = \big(S(t), R(t), M(t), G(t), C(t), A(t), O(t), E(t), F(t)\big)^{\mathrm{T}},$$
$$N_0 = (S_0, R_0, M_0, G_0, C_0, A_0, O_0, E_0, F_0)^{\mathrm{T}},$$
$$\Phi\big(t, N(t)\big) = (\Theta_1, \Theta_2, \Theta_3, \Theta_4, \Theta_5, \Theta_6, \Theta_7, \Theta_8, \Theta_9)^{\mathrm{T}}.$$

Lemma 1. (*See* [12].) *The solution of the problem*

$$^{C}D_t^{\eta} x(t) = g(t), \quad 0 < q \leqslant 1,$$
$$x(0) = x_0$$

is given by

$$x(t) = x_0 + \frac{1}{\Gamma(\eta)} \int_0^t (t-\xi)^{\eta-1} g(\xi)\,\mathrm{d}\xi.$$

By Lemma 1, the solution of system (2) satisfies the following equation:

$$N(t) = N_0 + \frac{1}{\Gamma(\eta)} \int_0^t (t-\xi)^{\eta-1} \Phi\big(\xi, N(\xi)\big)\,\mathrm{d}\xi. \tag{3}$$

Let $C_9[0,T] = \{N(t) \mid N(\cdot) : [0,T] \to R^9 \text{ is continuous}\}$, then C_9 is a Banach space with the norm $\|N\| = \sup_{0\leqslant t\leqslant T} |N(t)|$. Next, we define an operator $B : C_9[0,T] \to C_9[0,T]$ as follows:

$$BN(t) = N_0 + \frac{1}{\Gamma(\eta)} \int_0^t (t-\xi)^{\eta-1} \Phi\big(\xi, N(\xi)\big)\,\mathrm{d}\xi,$$

then the fixed point of operator B is the solution of Eq. (3).

In order to obtain the required theorem, we need the following assumptions:

($\mathcal{A}_1$) There exist positive functions $Z(t), I(t) \in L^q[0,T]$ with $q > 1/\eta$ such that

$$\big|\Phi\big(t, N(t)\big)\big| \leqslant Z(t)\big|N(t)\big|^{\alpha} + I(t),$$

where $\alpha > 0$;

($\mathcal{A}_2$) There exists a positive function $Q(t) \in L^q[0,T]$ with $q > 1/\eta$ such that

$$\big|\Phi\big(t, N(t)\big) - \Phi\big(t, \overline{N}(t)\big)\big| \leqslant Q(t)\big|N(t) - \overline{N}(t)\big|.$$

Next, we present the existence and uniqueness of the solution for the fractional SSF model.

Theorem 1. *Under assumption* ($\mathcal{A}_1$)*, the fractional SSF model* (1) *has at least one solution* $N(t) \in C_9[0,T]$ *such that*

$$\|N\| \leqslant \left(\|N_0\| + \frac{\|I\|_{L^1} T^{\eta}}{\Gamma(\eta+1)}\right) E_{\eta}\big(\|Z\|_{L^1} T^{\eta}\big) \quad \forall t \in [0,T].$$

Proof. Let us show that operator B is continuous. For $N(t) \in C_9$ with $\|N\| \leqslant k$,

$$\begin{aligned}
\big|BN(t)\big| &= \left|N_0 + \frac{1}{\Gamma(\eta)}\int_0^t (t-\xi)^{\eta-1}\Phi\big(\xi, N(\xi)\big)\,\mathrm{d}\xi\right| \\
&\leqslant |N_0| + \frac{1}{\Gamma(\eta)}\int_0^t (t-\xi)^{\eta-1}\big|\Phi\big(\xi, N(\xi)\big)\big|\,\mathrm{d}\xi \\
&\leqslant |N_0| + \frac{1}{\Gamma(\eta)}\left[\|Z\|_{L^q}\int_0^t \big((t-\xi)^{\eta-1}\big)^{q/(q-1)}\big|N(\xi)\big|^{\alpha}\,\mathrm{d}\xi\right. \\
&\quad \left. + \|I\|_{L^q}\int_0^t \big((t-\xi)^{\eta-1}\big)^{q/(q-1)}\,\mathrm{d}\xi\right] \\
&\leqslant |N_0| + \frac{k^{\alpha}\|Z\|_{L^q} + \|I\|_{L^q}}{\Gamma(\eta)}\int_0^t \big((t-\xi)^{\eta-1}\big)^{q/(q-1)}\,\mathrm{d}\xi \\
&\leqslant |N_0| + \frac{(k^{\alpha}\|Z\|_{L^q} + \|I\|_{L^q})(q-1)T^{(q\eta-1)/(q-1)}}{\Gamma(\eta)(q\eta-1)}. \qquad (4)
\end{aligned}$$

Hence, B is bounded. Let $0 < t_1 < t_2 < T$, one has

$$\begin{aligned}
&\big|BN(t_2) - BN(t_1)\big| \\
&= \left|\frac{1}{\Gamma(\eta)}\int_0^{t_2}(t_2-\xi)^{\eta-1}\Phi\big(\xi, N(\xi)\big)\,\mathrm{d}\xi - \frac{1}{\Gamma(\eta)}\int_0^{t_1}(t_1-\xi)^{\eta-1}\Phi\big(\xi, N(\xi)\big)\,\mathrm{d}\xi\right| \\
&\leqslant \frac{1}{\Gamma(\eta)}\int_0^{t_1}\big((t_2-\xi)^{\eta-1} - (t_1-\xi)^{\eta-1}\big)\big|\Phi\big(\xi, N(\xi)\big)\big|\,\mathrm{d}\xi \\
&\quad + \frac{1}{\Gamma(\eta)}\int_{t_1}^{t_2}(t_2-\xi)^{\eta-1}\big|\Phi\big(\xi, N(\xi)\big)\big|\,\mathrm{d}\xi \\
&\leqslant \frac{1}{\Gamma(\eta)}\left[\|Z\|_{L^q}\int_0^{t_1}\big((t_2-\xi)^{\eta-1} - (t_1-\xi)^{\eta-1}\big)\big|N(\xi)\big|^{\alpha}\,\mathrm{d}\xi\right. \\
&\quad \left. + \|I\|_{L^q}\int_0^{t_1}\big((t_2-\xi)^{\eta-1} - (t_1-\xi)^{\eta-1}\big)\,\mathrm{d}\xi\right] \\
&\quad + \frac{1}{\Gamma(\eta)}\left[\|Z\|_{L^q}\int_{t_1}^{t_2}(t_2-\xi)^{\eta-1}\big|N(\xi)\big|^{\alpha}\,\mathrm{d}\xi + \|I\|_{L^q}\int_{t_1}^{t_2}(t_2-\xi)^{\eta-1}\,\mathrm{d}\xi\right] \\
&\leqslant \frac{1}{\Gamma(\eta+1)}\big(k^{\alpha}\|Z\|_{L^q} + \|I\|_{L^q}\big)\big(t_2^{\eta} - t_1^{\eta}\big).
\end{aligned}$$

When $t_2 \to t_1$, it can be obtained that

$$\big\|BN(t_2) - BN(t_1)\big\| \to 0.$$

So, B is equicontinuous. According to the Arzelà–Ascoli theorem, it can be inferred that $B : C_9[0,T] \to C_9[0,T]$ is a completely continuous operator.

For $0 < \mu < 1$, $N(t) = \mu BN(t)$. Similar to the derivation of (4), there are

$$\begin{aligned}\big|N(t)\big| &= \big|\mu BN(t)\big| \\ &\leqslant \|N_0\| + \frac{\|I\|_{L^q}T^\eta}{\Gamma(\eta+1)} + \frac{\|Z\|_{L^q}}{\Gamma(\eta)}\int_0^t (t-\xi)^{\eta-1}\big|N(\xi)\big|^\alpha \,\mathrm{d}\xi.\end{aligned}$$

By applying the generalized Gronwall inequality [22], we have

$$\|N\| = \sup_{0\leqslant t\leqslant T}\big|N(t)\big| \leqslant \left(\|N_0\| + \frac{\|I\|_{L^q}T^\eta}{\Gamma(\eta+1)}\right)E_\eta\big(\|Z\|_{L^q}T^\eta\big),$$

where E_η is the Mittag-Leffer function defined by $E_\eta(u) = \sum_{n=0}^{\infty} u^n/\Gamma(n\eta+1)$.

According to the Leray–Schauder fixed point theorem, the fractional SSF model (1) has at least one solution $N(t) \in C_9[0,T]$ such that $\|N\| \leqslant (\|N_0\| + \|I\|_{L^q}T^\eta/\Gamma(\eta+1)) \times E_\eta(\|Z\|_{L^q}T^\eta)$. □

Theorem 2. *Under assumption* $(\mathcal{A}_2)$*, if* $T^\eta\|Q\|_{L^1}/\Gamma(\eta+1) < 1$*, then the fractional SSF model* (1) *has a unique positive solution.*

Proof. For $N(t), \overline{N}(t) \in C_9[0,T]$, there are

$$\begin{aligned}&\big|BN(t) - B\overline{N}(t)\big| \\ &\quad= \left|\frac{1}{\Gamma(\eta)}\int_0^t (t-\xi)^{\eta-1}\Phi\big(\xi, N(\xi)\big)\,\mathrm{d}\xi - \frac{1}{\Gamma(\eta)}\int_0^t (t-\xi)^{\eta-1}\Phi\big(\xi, \overline{N}(\xi)\big)\,\mathrm{d}\xi\right| \\ &\quad\leqslant \frac{1}{\Gamma(\eta)}\int_0^t (t-\xi)^{\eta-1}\big|\Phi\big(\xi, N(\xi)\big) - \Phi\big(\xi, \overline{N}(\xi)\big)\big|\,\mathrm{d}\xi \\ &\quad\leqslant \frac{\|Q\|_{L^1}}{\Gamma(\eta)}\int_0^t (t-\xi)^{\eta-1}\big|N(t) - \overline{N}(t)\big|\,\mathrm{d}\xi \leqslant \frac{T^\eta\|Q\|_{L^1}}{\Gamma(\eta+1)}\|N - \overline{N}\|.\end{aligned}$$

Since $T^\eta\|Q\|_{L^1}/\Gamma(\eta+1) < 1$, then $\|BN - B\overline{N}\| < \|N - \overline{N}\|$. Hence, the fractional SSF model (1) has a unique solution by using the Banach contraction theorem. Similar to the proof of Theorem 2.1 in [13], it is easy to prove that the solution of the fractional SSF model we proposed is positive. □

Next, we analyze the stability of the fractional SSF model at the equilibrium point.

Definition 1. (See [16].) A point x^* is called to be an equilibrium point of the system

$$^{C}D_t^{\eta}x(t) = f\big(t, x(t)\big), \quad \eta \in (0,1),$$

if and only if $f(t, x^*) = 0$.

Lemma 2. (*See* [6].) *The equilibrium point $x = 0$ of $\dot{x} = Ax$ is stable if and only if all eigenvalues of A satisfy $\mathrm{Re}[\lambda_i] \leqslant 0$ and for every eigenvalue with $\mathrm{Re}[\lambda_i] = 0$ and algebraic multiplicity $q_i \geqslant 2$, $\mathrm{rank}(A - \lambda_i I) = n - q_i$, where n is the dimension of x, and q_i is the multiplicity of λ_i when $\lambda_i = 0$ in $\det(\lambda_i I - A)$.*

Theorem 3. *The fractional SSF model* (1) *is stable at the equilibrium point.*

Proof. Let $^{C}D^{\eta}N(t) = 0$. The equilibrium point of the fractional SSF model (1) can be calculated as $\mathcal{D}_0 = (0,0,0,0,0,0,0,0,0)$ and $\mathcal{D}_1 = (0,0,0,0,0,0,-(k_9 + k_{s2} + k_{s5})/(k_8 + k_{s6} + k_9 k_{s5}), 0, 0)$. We further calculate the Jacobian matrix of the fractional SSF model (1) at the equilibrium point as follows:

$$\mathcal{J}_{\mathcal{D}_0} = \mathcal{J}_{\mathcal{D}_1} = \begin{pmatrix} 0 & 0 & 0 & 0 & 0 & 0 & 0 & 0 & 0 \\ 0 & 0 & 0 & 0 & 0 & 0 & 0 & 0 & k_{10} \\ 0 & 0 & 0 & 0 & 0 & 0 & 0 & 0 & k_{11} \\ 0 & 0 & 0 & 0 & 0 & 0 & 0 & 0 & k_{12} \\ 0 & 0 & 0 & 0 & 0 & 0 & 0 & 0 & 0 \\ 0 & 0 & 0 & 0 & 0 & 0 & 0 & 0 & 0 \\ 0 & 0 & 0 & 0 & 0 & 0 & 0 & 0 & 0 \\ 0 & 0 & 0 & 0 & 0 & 0 & 0 & 0 & k_2 + k_3 + k_4 \\ 0 & 0 & 0 & 0 & 0 & 0 & 0 & 0 & -(k_2 + k_3 + k_4) \end{pmatrix}.$$

We evaluate the characteristic equation depending on λ of $\mathcal{J}_{\mathcal{D}^0}$ as given below:

$$\lambda^9 + (k_2 + k_3 + k_4)\lambda^8 = 0.$$

It is easy to see that all eigenvalues of matrix $\mathcal{J}_{\mathcal{D}^0}$ satisfy $\mathrm{Re}[\lambda_i] \leqslant 0$. Among them, the eight multiplicity eigenvalues of $\mathcal{J}_{\mathcal{D}^0}$ are 0, and the other one is less than 0. At the same time, the following formula holds:

$$\mathrm{rank}(A - 0I) = 9 - 8 = 1.$$

According to Lemma 2, the fractional SSF model is stable at the equilibrium point. □

Next, in order to comprehensively and deeply understand the dynamic characteristics of the fractional SSF model of rice wine, ensure the reliability of this model on a long-time scale and improve the accuracy of predicting the system trends, the Ulam–Hyers stability and the generalized Ulam–Hyers stability of the fractional SSF model are analyzed. Let ε satisfy the following inequality:

$$\big|^{C}D^{\eta}N(t) - \Phi\big(t, N(t)\big)\big| \leqslant \varepsilon, \tag{5}$$

where $t \in [0,T]$, $\varepsilon = \max(\varepsilon_j)^{\mathrm{T}} > 0$, $j = 1, 2, \ldots, 9$.

Definition 2. (See [1].) Assume that $\widetilde{N}(t) \in C_9$ satisfies (5) and $N(t) \in C_9$ is the unique solution of (2). For any $\varepsilon > 0$, if there exists $U_\Phi > 0$ such that

$$\left|\widetilde{N}(t) - N(t)\right| \leqslant U_\Phi \varepsilon, \quad t \in [0,T],$$

where $U_\Phi = \max(U_{\Phi_j})^{\mathrm{T}}$, $j = 1,2,\ldots,9$, then the fractional SSF model (1) is Ulam–Hyers stable.

Definition 3. (See [5].) Assume that $\widetilde{N}(t) \in C_9$ satisfies (5) and $N(t) \in C_9$ is the unique solution of (2). For any $\varepsilon > 0$, if there exist a continuous function $\mathcal{W} : R^+ \to R^+$ and $\mathcal{W}(0) = 0$ such that

$$\left|\widetilde{N}(t) - N(t)\right| \leqslant \mathcal{W}_\Phi(\varepsilon), \quad t \in [0,T],$$

where $\mathcal{W}_\Phi = \max(\mathcal{W}_{\Phi_j})^{\mathrm{T}}$, $j = 1,2,\ldots,9$, then the fractional SSF model (1) is generalized Ulam–Hyers stable.

Remark 1. A function $\widetilde{N}(t) \in C_9$ satisfies (5) if and only if there exists a function $v(t) \in C_9$ with the following properties:

(i) $|v(t)| \leqslant \varepsilon$, $t \in [0,T]$.

(ii) ${}^{C}D^{\eta}\widetilde{N}(t) = \Phi(t,\widetilde{N}(t)) + v(t)$, $t \in [0,T]$.

Theorem 4. *Under assumption* $(\mathcal{A}_2)$*, if* $\Gamma(\eta+1) > T^\eta \|Q\|_{L^1}$*, then the fractional SSF model* (1) *is Ulam–Hyers stable and generalized Ulam–Hyers stable.*

Proof. If $\widetilde{N}(t)$ satisfies the inequality given by (5) and $N(t)$ is a unique solution of (2), then for all $\varepsilon > 0$, $t \in [0,T]$, together with Remark 1, we have

$$\begin{aligned}
&\left|\widetilde{N}(t) - N(t)\right| \\
&\quad = \left| \frac{1}{\Gamma(\eta)} \int_0^t (t-\xi)^{\eta-1} \big(\Phi\big(\xi,\widetilde{N}(\xi)\big) + v(\xi)\big)\,\mathrm{d}\xi - \frac{1}{\Gamma(\eta)} \int_0^t (t-\xi)^{\eta-1} \Phi\big(\xi,N(\xi)\big)\,\mathrm{d}\xi \right| \\
&\quad \leqslant \frac{1}{\Gamma(\eta)} \int_0^t (t-\xi)^{\eta-1} \big|v(\xi)\big|\,\mathrm{d}\xi + \frac{1}{\Gamma(\eta)} \int_0^t (t-\xi)^{\eta-1} \big|\Phi\big(\xi,\widetilde{N}(\xi)\big) - \Phi\big(\xi,N(\xi)\big)\big|\,\mathrm{d}\xi \\
&\quad \leqslant \frac{T^\eta}{\Gamma(\eta+1)}\varepsilon + \frac{T^\eta}{\Gamma(\eta+1)} \|Q\|_{L^1} \|\widetilde{N} - N\|.
\end{aligned}$$

Thus, we have

$$\|\widetilde{N} - N\| \leqslant U_\Phi \varepsilon, \tag{6}$$

where $U_\Phi = T^\eta/(\Gamma(\eta+1) - T^\eta\|Q\|_{L^1})$. By Definition 2, the fractional SSF model (1) is Ulam–Hyers stable. In (6), if we take $\mathcal{W}_\Phi(\varepsilon) = U_\Phi\varepsilon$, then $\mathcal{W}_\Phi(0) = 0$. According to Definition 3, the fractional SSF model (1) is generalized Ulam–Hyers stable. □

3 Numerical simulation of fractional SSF model

In this section, we give the approximate solution of the fractional SSF model (1). Then numerical simulations are carried out with the proposed method.

Here we apply the generalised Euler method in [2] to the fractional SSF model (1). Let $[0, a]$ be the interval of solution for problem (2). We subdivide the interval $[0, a]$ into q subintervals $[t_q, t_{q+1}]$ by using the nodes $t_q = qh$, where $h = a/m$ represents the length of subintervals, $q = 0, 1, 2 \ldots, m-1$. By using the generalized Euler method, the iterative form of $N(t)$ at $t_{q+1} = t_q + h$ is

$$
\begin{aligned}
S(t_{q+1}) &= S(t_q) + \Theta_1\big(S(t_q), R(t_q), M(t_q), G(t_q), C(t_q), A(t_q), O(t_q), E(t_q), F(t_q)\big) \\
&\quad \times \frac{h^\eta}{\Gamma(\eta+1)}, \\
R(t_{q+1}) &= S(t_q) + \Theta_2\big(S(t_q), R(t_q), M(t_q), G(t_q), C(t_q), A(t_q), O(t_q), E(t_q), F(t_q)\big) \\
&\quad \times \frac{h^\eta}{\Gamma(\eta+1)}, \\
M(t_{q+1}) &= S(t_q) + \Theta_3\big(S(t_q), R(t_q), M(t_q), G(t_q), C(t_q), A(t_q), O(t_q), E(t_q), F(t_q)\big) \\
&\quad \times \frac{h^\eta}{\Gamma(\eta+1)}, \\
G(t_{q+1}) &= G(t_q) + \Theta_4\big(S(t_q), R(t_q), M(t_q), G(t_q), C(t_q), A(t_q), O(t_q), E(t_q), F(t_q)\big) \\
&\quad \times \frac{h^\eta}{\Gamma(\eta+1)}, \\
C(t_{q+1}) &= C(t_q) + \Theta_5\big(S(t_q), R(t_q), M(t_q), G(t_q), C(t_q), A(t_q), O(t_q), E(t_q), F(t_q)\big) \\
&\quad \times \frac{h^\eta}{\Gamma(\eta+1)}, \\
A(t_{q+1}) &= A(t_q) + \Theta_6\big(S(t_q), R(t_q), M(t_q), G(t_q), C(t_q), A(t_q), O(t_q), E(t_q), F(t_q)\big) \\
&\quad \times \frac{h^\eta}{\Gamma(\eta+1)}, \\
O(t_{q+1}) &= O(t_q) + \Theta_7\big(S(t_q), R(t_q), M(t_q), G(t_q), C(t_q), A(t_q), O(t_q), E(t_q), F(t_q)\big) \\
&\quad \times \frac{h^\eta}{\Gamma(\eta+1)}, \\
E(t_{q+1}) &= E(t_q) + \Theta_8\big(S(t_q), R(t_q), M(t_q), G(t_q), C(t_q), A(t_q), O(t_q), E(t_q), F(t_q)\big) \\
&\quad \times \frac{h^\eta}{\Gamma(\eta+1)}, \\
F(t_{q+1}) &= F(t_q) + \Theta_9\big(S(t_q), R(t_q), M(t_q), G(t_q), C(t_q), A(t_q), O(t_q), E(t_q), F(t_q)\big) \\
&\quad \times \frac{h^\eta}{\Gamma(\eta+1)},
\end{aligned}
$$

where $q = 0, 1, 2, \ldots, m-1$.

It can be written as

$$N(t_{q+1}) = N(t_q) + \frac{h^\eta}{\Gamma(\eta+1)}\Phi\big(t_q, N(t_q)\big).$$

The exact solution of the fractional SSF model is as follows:

$$\begin{aligned} N^*(t_{q+1}) &= N_0 + \frac{1}{\Gamma(\eta)}\int_0^{t_{q+1}} (t_{q+1}-\xi)^{\eta-1}\Phi\big(\xi, N^*(\xi)\big)\,\mathrm{d}\xi. \\ &= N_0 + \frac{1}{\Gamma(\eta)}\int_0^{t_q} (t_{q+1}-\xi)^{\eta-1}\Phi\big(\xi, N^*(\xi)\big)\,\mathrm{d}\xi \\ &\quad + \frac{1}{\Gamma(\eta)}\int_{t_q}^{t_{q+1}} (t_{q+1}-\xi)^{\eta-1}\Phi\big(\xi, N^*(\xi)\big)\,\mathrm{d}\xi. \end{aligned}$$

For $(1/\Gamma(\eta))\int_{t_q}^{t_{q+1}}(t_{q+1}-\xi)^{\eta-1}\Phi(\xi, N^*(\xi))\,\mathrm{d}\xi$, by using the mean value theorem of integrals, there exists $\xi_q \in (t_q, t_{q+1})$ such that

$$\frac{1}{\Gamma(\eta)}\int_{t_q}^{t_{q+1}} (t_{q+1}-\xi)^{\eta-1}\Phi\big(\xi, N^*(\xi)\big)\,\mathrm{d}\xi = \frac{h^\eta}{\Gamma(\eta+1)}\Phi\big(\xi_q, N^*(\xi_q)\big).$$

Thus,

$$e_{q+1} = N^*(t_{q+1}) - N(t_{q+1}) = e_q + \frac{h^\eta}{\Gamma(\eta+1)}\big[\Phi\big(\xi_q, N^*(\xi_q)\big) - \Phi\big(t_q, N(t_q)\big)\big],$$

$$\begin{aligned} |e_{q+1}| &\leqslant |e_q| + \frac{h^\eta}{\Gamma(\eta+1)}\big[\big|\Phi\big(\xi_q, N^*(\xi_q)\big) - \Phi\big(\xi_q, N(t_q)\big)\big| \\ &\quad + \big|\Phi\big(\xi_q, N(t_q)\big) - \Phi\big(t_q, N(t_q)\big)\big|\big] \\ &\leqslant |e_q| + \frac{h^\eta}{\Gamma(\eta+1)}\big[L\big|N^*(\xi_q) - N(t_q)\big| + \big|\Phi\big(\xi_q, N(t_q)\big) - \Phi\big(t_q, N(t_q)\big)\big|\big] \\ &\leqslant |e_q| + Ch^\eta|e_q| + O\big(h^{\eta+1}\big) = \big(1+Ch^\eta\big)|e_q| + O\big(h^{\eta+1}\big). \end{aligned}$$

When $q=0$, e_0 is the initial error. Suppose $e_q \leqslant M(1+Ch^\eta)^q|e_0| + O(h^\eta)$, then

$$\begin{aligned} |e_{q+1}| &\leqslant \big(1+Ch^\eta\big)\big[M(1+Ch^\eta)^q|e_0| + O(h^\eta)\big] + O\big(h^{\eta+1}\big) \\ &= M\big(1+Ch^\eta\big)^{q+1}|e_0| + O\big(h^\eta\big). \end{aligned}$$

When $h \to 0$, $(1+Ch^\eta)^{q+1} \to 1$, so $\lim_{h\to 0}|e_{q+1}| = 0$, meaning that the numerical method converges.

Table 2. Initial values of each substrate concentration [9].

Substrate concentration	Initial value [g/L]	Substrate concentration	Initial value [g/L]
$S(0)$	151.68	$A(0)$	0
$R(0)$	0	$O(0)$	0.042
$M(0)$	0	$E(0)$	24.26
$G(0)$	0	$F(0)$	0
$C(0)$	5.6		

Table 3. Estimated values of the model parameters [9].

Parameter	Value	Parameter	Value	Parameter	Value
k_1	0.007	k_9	0.062	k_{17}	0.032
k_2	1.695	k_{10}	1.758	K_{s1}	5.970
k_3	20.818	k_{11}	21.984	K_{s2}	6.900
k_4	0.685	k_{12}	0.761	K_{s3}	30.900
k_5	0.643	k_{13}	0.054	K_{s4}	30.500
k_6	2.929	k_{14}	0.258	K_{s5}	6.315
k_7	0.886	k_{15}	0.037	K_{s6}	6.315
k_8	0.412	k_{16}	0.476		

The local truncation error is $T_{q+1} = O(h^{\eta+1})$,

$$|e_{q+1}| \leqslant \big(1 + Ch^{\eta}\big)|e_q| + |T_{q+1}|,$$

$$\begin{aligned} |e_q| &\leqslant \big(1 + Ch^{\eta}\big)^q |e_0| + \sum_{k=0}^{q-1} \big(1 + Ch^{\eta}\big)^k |T_{k+1}| \\ &= \big(1 + Ch^{\eta}\big)^q |e_0| + \frac{(1 + Ch^{\eta})^q - 1}{Ch^{\eta}} + O\big(h^{\eta+1}\big). \end{aligned}$$

When h is sufficiently small, $(1 + Ch^{\eta})^q \approx 1 + qCh^{\eta}$, then the overall error bound is

$$\begin{aligned} |e_q| &\leqslant \big(1 + qCh^{\eta}\big)|e_0| + \frac{1 + qCh^{\eta} - 1}{Ch^{\eta}} O\big(h^{\eta+1}\big) \\ &= \big(1 + qCh^{\eta}\big)|e_0| + qO\big(h^{\eta+1}\big). \end{aligned}$$

Based on previous research, it can be recognized that 28 °C is the most suitable temperature for rice wine fermentation [15]. The initial values and parameter values at 28 °C is shown in Tables 2 and 3.

During the fermentation process, the concentration of reactants usually decreases rapidly, especially, in the early stages of the reaction. Such rapid changes may lead to instability and computational difficulties in numerical simulations. In contrast, the concentration of product changes relatively slow, which makes it easier to perform numerical simulations. Therefore, the following numerical simulations will be conducted around four main products, maltotriose, maltose, glucose, and ethanol. The concentration changes of maltotriose, maltose, glucose, and ethanol with time in the fractional SSF model are shown in Figs. 1(a)–1(d), respectively. The y-axis represents the material concentration in g/L, and the x-axis represents the time in h. The blue line in Figs. 1(a)–1(d)

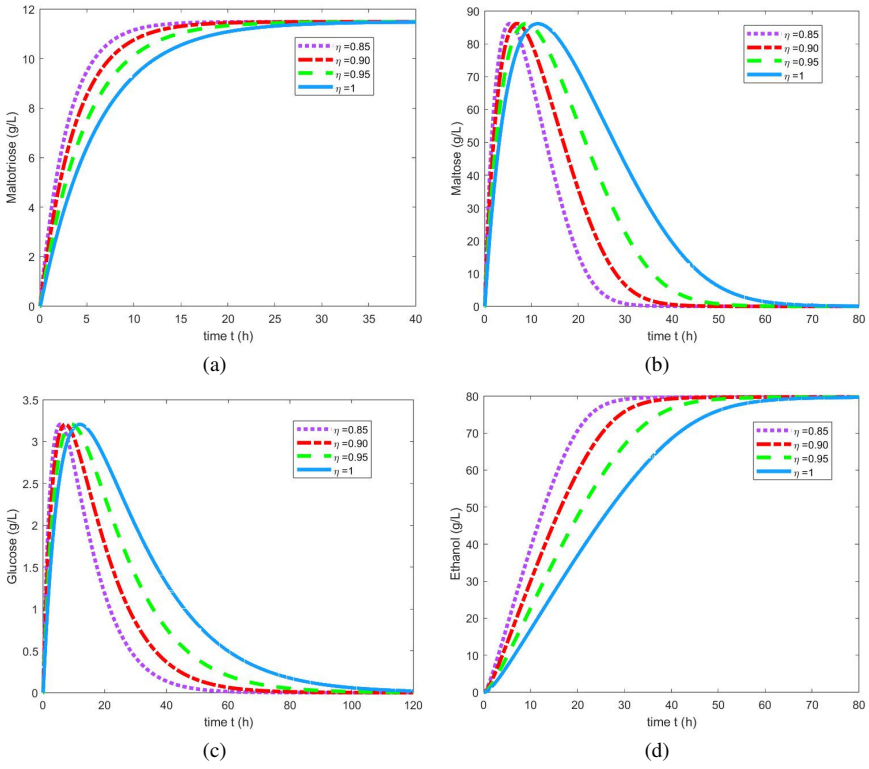

Figure 1. The variation of maltotriose (a), maltose (b), glucose (c), and ethanol (d) concentration with time. The blue line represents the variation of concentration with time when the order $\eta = 1$. The green, red, and purple lines represent the variation of concentration with time when the order η takes 0.95, 0.90, and 0.85, respectively.

represents the concentration changes of maltotriose, maltose, glucose, and ethanol with time when the order $\eta = 1$; the green, red, and purple lines represent the concentration changes of maltotriose, maltose, glucose, and ethanol with time when $\eta = 0.95$ (green), 0.90 (red), and 0.85 (purple).

Figure 1(a) shows that the concentration of maltotriose increases over time. When its concentration reaches 11.4902 g/L, it no longer changes with time.

Figures 1(b) and 1(c) show that the concentrations of maltose and glucose increase sharply with a short time and reach their peaks, then gradually decrease until reach zero. The smaller the order η is, the earlier the concentrations of maltose and glucose reach their peaks.

Figure 1(d) shows that the concentration of ethanol first increases and then stabilizes when it concentration reaches about 79.773 g/L. From Figs. 1(a)–1(d) the concentrations of maltotriose, maltose, glucose, and ethanol increase first and the concentrations of maltotriose, maltose, and glucose increase faster than the concentration of ethanol. Because first starch decomposes into maltotriose, maltose and glucose, then maltose

and glucose are metabolized into ethanol. Also, for this reason, the concentration of maltotriose reaches stability faster than the concentration of ethanol. The maltotriose decomposed by starch has a different trend compared to maltose and glucose because it is only used for the growth and maintenance of yeast.

From Figs. 1(a)–1(d) the smaller the order η, the faster the change rate. Taking Fig. 1(d) as an example, we analyze the change rate of ethanol concentration from $t_1 = 8.35$ to $t_2 = 8.55$. During this period, the concentration of ethanol is increasing. When $t_1 = 8.35$, the concentration of ethanol in the fractional SSF model is 32.3114, 24.5965, 18.4503, and 13.6466 when the order η is taken as 0.85, 0.90, 0.95, and 1, respectively. When $t_1 = 8.55$, the concentration of ethanol in the fractional SSF model is 33.1425, 25.2621, 18.9718, and 14.0483 when the order η is taken as 0.85, 0.90, 0.95, and 1, respectively. It can be calculated that the change rate of ethanol concentration during the period $[8.35, 8.55]$ is 4.1555, 3.328, 2.6075, and 2.0085 when the order η is taken as 0.85, 0.90, 0.95, and 1, respectively. It can be seen that the change rate of ethanol concentration at fractional order is faster than that at integer order. Furthermore, with the increase of the order, the change rate of ethanol concentration gradually approaches that of the integer order. The smaller the order, the relatively faster the change rate. Similar results for maltotriose, maltose, and glucose can be obtained from Figs. 1(a)–1(c). Therefore, the fractional SSF model can more sensitively capture changes in reaction.

4 Conclusion

During the fermentation process of rice wine, the concentration of substances changes with time. Because fractional derivatives can better consider the memory effect of the reaction system, they are more suitable to study the SSF process of rice wine. Therefore, in this paper, a fractional SSF model was proposed. Firstly, the existence and uniqueness of the solution for the fractional SSF model were given. Secondly, the Ulam–Hyers stability and the stability at the equilibrium point of the fractional SSF model were analyzed. Finally, the numerical simulations of the fractional SSF model were presented. Compared to integer order, fractional order can perceive changes in the reaction more detail. The fractional SSF model provides a new analysis tool for rice wine makers. It can help rice wine brewers to better control the brewing process and improve product quality.

References

1. Q.T. Ain, N. Anjum, A. Din, A. Zeb, S. Djilali, Z.A. Khan, On the analysis of Caputo fractional order dynamics of Middle East Lungs Coronavirus (MERS-CoV) model, *Alexandria Eng. J.*, **61**(7):5123–5131, 2022, https://doi.org/10.1016/j.aej.2021.10.016.
2. A. Arafa, S. Rida, M. Khalil, Fractional modeling dynamics of HIV and CD4+ T-cells during primary infection, *Nonlinear Biomed. Phys.*, **6**(1):1, 2012, https://doi.org/10.1186/1753-4631-6-1.
3. N. Huang, G. Wang, T. Guan, The dynamics analysis of a new wine fermentation model, *J. Appl. Math. Comput.*, **70**:3731–3747, 2024, https://doi.org/10.1007/s12190-024-02106-3.

4. M.A. Imran, N.A. Shah, I. Khan, M. Aleem, Applications of non-integer Caputo time fractional derivatives to natural convection flow subject to arbitrary velocity and Newtonian heating, *Neural Comput. Appl.*, **30**:1589–1599, 2018, https://doi.org/10.1007/s00521-016-2741-6.
5. D. Kang, H. Kim, Generalized Hyers–Ulam stability of diffusion equation in the n-dimensional Euclidean space $\mathbb{R}^n$, *Appl. Math. Lett.*, **103**:106169, 2020, https://doi.org/10.1016/j.aml.2019.106169.
6. H.K. Khalil, Lyapunov's stability theory, in J. Baillieul, T. Samad (Eds.), *Encyclopedia of Systems and Control*, Springer, Cham, 2021, https://doi.org/10.1007/978-3-030-44184-5_77.
7. A.D. Kroumov, A.N. Módenes, M.C. de Araujo Tait, Development of new unstructured model for simultaneous saccharification and fermentation of starch to ethanol by recombinant strain, *Biochem. Eng. J.*, **28**(3):243–255, 2006, https://doi.org/10.1016/j.bej.2005.11.008.
8. D. Liu, H. Zhang, C.-C. Lin, B. Xu, Optimization of rice wine fermentation process based on the simultaneous saccharification and fermentation kinetic model, *Chin. J. Chem. Eng.*, **24**(10):1406–1412, 2016, https://doi.org/10.1016/j.cjche.2016.05.037.
9. D. Liu, H. Zhang, B. Xu, J. Tan, Development of a kinetic model structure for simultaneous saccharification and fermentation in rice wine production, *J. Inst. Brew.*, **121**(4):589–596, 2015, https://doi.org/10.1002/jib.270.
10. S. Ochoa, A. Yoo, J.-U. Repke, G. Wozny, D.R. Yang, Modeling and parameter identification of the simultaneous saccharification fermentation process for ethanol production, *Biotechnol. Progr.*, **23**(6):1454–1462, 2007, https://doi.org/10.1021/bp0702119.
11. A. Padder, L. Ausif, S. Qureshi, A. Soomro, Dynamical analysis of generalized tumor model with Caputo fractional-order derivative, *Fractal Fract.*, **7**(3):258, 2023, https://doi.org/10.3390/fractalfract7030258.
12. K. Shah, A. Ali, S. Zeb, A. Khan, M.A. Alqudah, T. Abdeljawad, Study of fractional order dynamics of nonlinear mathematical model, *Alexandria Eng. J.*, **61**(12):11211–11224, 2022, https://doi.org/10.1016/j.aej.2022.04.039.
13. R. Shi, C. Zhao, Stability, Hopf bifurcation and control of a fractional order delay cervical cancer model with HPV infection, *Comput. Methods Biomech. Biomed. Eng.*, **8**:1–25, 2025, https://doi.org/10.1080/10255842.2025.2457601.
14. J. Singh, D. Kumar, M. Al Qurashi, D. Baleanu, A new fractional model for giving up smoking dynamics, *Adv. Difference Equ.*, **2017**:88, 2017, https://doi.org/10.1186/s13662-017-1139-9.
15. M.J. Torija, N. Rozés, M. Poblet, J.S. Guillamón, A. Mas, Effects of fermentation temperature on the strain population of Saccharomyces cerevisiae, *Int. J. Food Microbiol.*, **80**(1):47–53, 2003, https://doi.org/10.1016/S0168-1605(02)00144-7.
16. S. Ullah, M. Altanji, M.A. Khan, A. Alshaheri, W. Sumelka, The dynamics of HIV/AIDS model with fractal-fractional Caputo derivative, *Fractals*, **31**(2):2340015, 2023, https://doi.org/10.1142/S0218348X23400157.
17. P. Wang, J. Mao, X. Meng, X. Li, Y. Liu, H. Feng, Changes in flavour characteristics and bacterial diversity during the traditional fermentation of Chinese rice wines from Shaoxing region, *Food Control*, **44**:58–63, 2014, https://doi.org/10.1016/j.foodcont.2014.03.018.

18. R. Wang, R. Koppram, L. Olsson, C.J. Franzén, Kinetic modeling of multi-feed simultaneous saccharification and co-fermentation of pretreated birch to ethanol, *Bioresour. Technol.*, **172**: 303–311, 2014, https://doi.org/10.1016/j.biortech.2014.09.028.

19. X.L. Wei, S.P. Liu, J.S. Yu, Y.J. Yu, S.H. Zhu, Z.L. Zhou, J. Hu, J. Mao, Innovation Chinese rice wine brewing technology by bi-acidification to exclude rice soaking process, *J. Biosci. Bioeng.*, **123**(4):460–465, 2017, https://doi.org/10.1016/j.jbiosc.2016.11.014.

20. E. Wua, J. Zhu, Y. Sun, S. He, A general plastic model for rockfill material developed by using Caputo fractional derivative, *Comput. Geotech.*, **151**:104948, 2022, https://doi.org/10.1016/j.compgeo.2022.104948.

21. J. Xu, H. Wu, Z. Wang, F. Zheng, X. Lu, Z. Li, Q. Ren, Microbial dynamics and metabolite changes in Chinese rice wine fermentation from sorghum with different tannin content, *Sci. Rep.*, **8**:4639, 2018, https://doi.org/10.1038/s41598-018-23013-1.

22. H. Ye, J. Gao, Y. Ding, A generalized Gronwall inequality and its application to a fractional differential equation, *J. Math. Anal. Appl.*, **328**(2):1075–1081, 2007, https://doi.org/10.1016/j.jmaa.2006.05.061.

23. L. Yu, F. Ding, H. Ye, Analysis of characteristic flavour compounds in Chinese rice wines and representative fungi in wheat *Qu* samples from different regions, *J. Inst. Brew.*, **118**(1):114–119, 2012, https://doi.org/10.1002/jib.13.

24. K. Zhang, Q. Li, W. Wu, J. Yang, W. Zhou, Wheat qu and its production technology, microbiota, flavor, and metabolites, *J. Food Sci.*, **84**(9):2373–2386, 2019, https://doi.org/10.1111/1750-3841.14768.

25. L. Zhang, N. Qin, B. Ahmad, Explicit iterative solution of a Caputo–Hadamard-type fractional turbulent flow model, *Math. Methods Appl. Sci.*, **47**(13):10548–10558, 2020, https://doi.org/10.1002/mma.6277.

26. L. Zhou, F.S. Alenezi, A. Nandal, A. Dhaka, T. Wu, D. Koundal, A. Alhudhaif, K. Polat, Fusion of overexposed and underexposed images using Caputo differential operator for resolution and texture based enhancement, *Appl. Intell.*, **53**(12):15836–15854, 2023, https://doi.org/10.1007/s10489-022-04344-z.